Cortical Recording with Conducting Polymer Electrodes

by

Woong Jin Bae

B.S. Mechanical Engineering
University of California, Los Angeles, 2006

Submitted to the Department of Mechanical Engineering
In Partial Fulfillment of the Requirements of the Degree of

Masters of Science in Mechanical Engineering

at the

Massachusetts Institute of Technology

June 2008

Signature of Author..........................

<div align="right">

Department of Mechanical Engineering
May 15, 2008

</div>

Certified by..

<div align="right">

Emilio Bizzi
Institute Professor
Thesis Supervisor

</div>

Certified by..

<div align="right">

Ian W. Hunter
Hatsopoulos Professor of Mechanical Engineering
Thesis Co-Supervisor

</div>

Accepted by......................................

<div align="right">

Lallit Anand
Professor of Mechanical Engineering
Chairman, Department Committee on Graduate Students

</div>

1
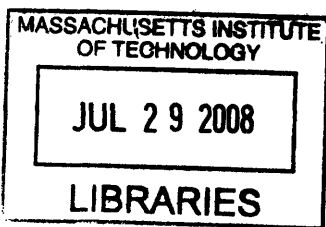
Cortical Recording with Conducting Polymer Electrodes

by

Woong Jin Bae

Submitted to the Department of Mechanical Engineering
on May 15th, 2008 in Partial Fulfillment of the Requirements
for the degree of Master of Science in Mechanical Engineering

ABTRACT

The ability to record from the same neuron for extended periods of time is essential to understanding how the brain reorganizes during motor learning. Conventional chronic recording microelectrodes are made from metal or silicon. However, the large stiffness mismatch between the electrodes and brain tissue causes shear-induced inflammation, limiting long-term recording stability. The flexibility of a polypyrrole microwire has the potential to improve the chronic recording stability by minimizing the stiffness mismatch. This thesis shows the fabrication of conducting polymer electrodes and the stability of their impedance in physiological saline. The initial impedance was as low as 70 kΩ, but the electrode impedance increased by a factor of 10 when immersed in saline over 370 hours. This conducting polymer microwire electrode was implanted in a rodent brain and successfully used to record neuronal action potentials.

Thesis Supervisor: Emilio Bizzi
Title: Institute Professor

Thesis Co-Supervisor: Ian W. Hunter
Title: Hatsopoulos Professor of Mechanical Engineering

Acknowledgements

First of all, I would like to thank my two advisors, Professor Emilio Bizzi and Professor Ian Hunter for their support and guidance throughout my Master's work.

I would also like to thank all my colleagues in the Bizzi lab and in the Bioinstrumentation lab and am especially grateful to Andrew Richardson and Bryan Ruddy.

I would also like to thank the KGSA-ME members and the SB family including HyeSung Park, Sungho Lee, Sungmin Son.

Lastly, I would like to thank my parents and my younger brother.

TABLE OF CONTENTS

List of Figures

Chapter 1.   Introduction

1.1   Motivation

Cortical neural electrodes provide an interface to the nervous system, converting physiological activities of neurons to electrical signals. Intracortical recordings can provide cellular-level resolution of neuronal activities, which is not attainable with non-invasive methods (Cheung, 2007). Cortical recordings have contributed to the identification of brain functions such as reasoning, planning, motor learning, speech, emotions, recognition, auditory and visual processing, and memory (Bear et al., 2007). Figure 1 illustrates the locations of these major brain functions of the cortex.
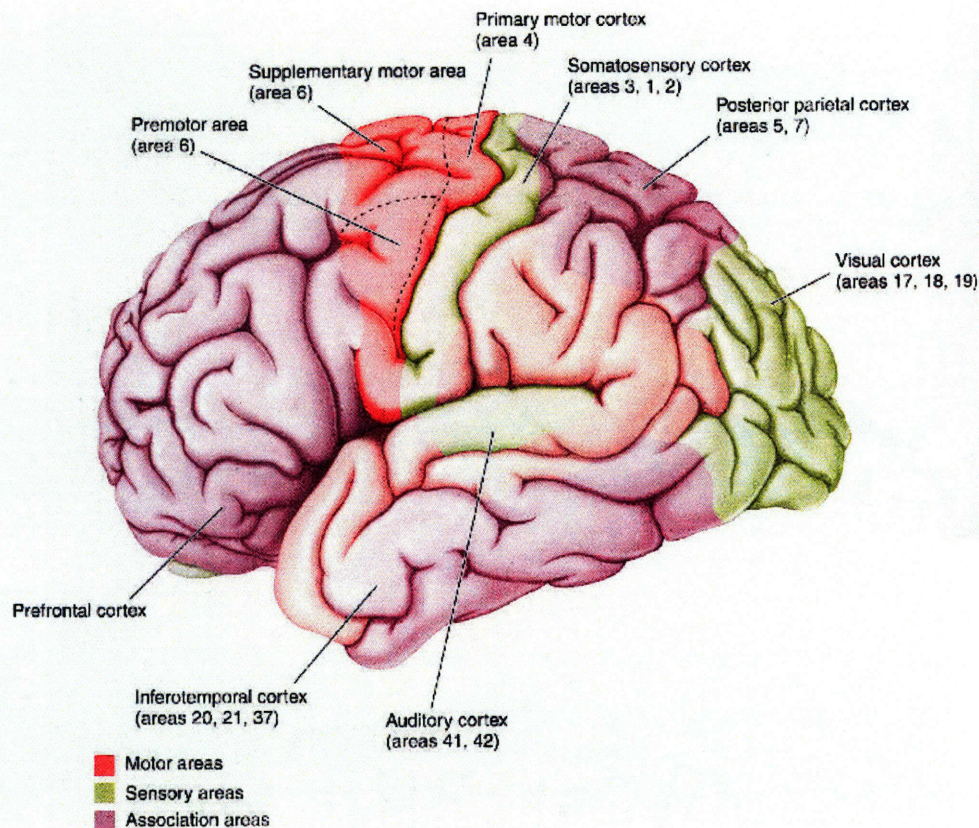

Figure 1. Major Areas of Cortex (from Bear et al., 2007).

System-level mechanisms of these brain functions are challenging to investigate, especially for learning. Understanding learning mechanisms requires characterizing the activities of individual neurons and the interactions across populations of neurons for an extended period of time (Tolias et al., 2007). A stable chronic cortical recording, which can track activities of multiple and identifiable single neurons over time, is essential to investigating motor learning.

1.2 Chronic Cortical Electrodes

The cerebral cortex is the outer-most layer of the brain, and has a density of approximately 3×10^{13} neurons/m^3. Pyramidal neurons are among the largest cells (cell bodies of 10-30 μm in diameter) and represent 80% of all cortical neurons. Ideally, chronic cortical electrodes should establish a sensitive and stable interface with these neurons, and record from the same cells for an extended period of time. In order to isolate single neuronal activity, the recording site should be similar in size to a cell body (Kipke et al., 2004).

Material selection for electrodes is a critical issue. It is important not only to prevent a significant host reaction towards the implant, but also to maintain good signal quality. The materials for both the electrode and its insulation should be biocompatible and inert to brain tissue. Commonly used materials for electrodes are platinum, iridium, and tungsten because they have high electrical conductivity, low chemical reactivity, and high resistance to corrosion.

One of the first chronic neural recording techniques was the use of insulated metal microwires. Simply cutting the end of the wire exposed a conductive recording site. Strumwasser used several 80 μm diameter stainless-steel microwires to record neural activities from the brains of squirrels for weeks (Strumwasser, 1958). Marg et al. and Burns et al. improved this method by etching microwires to a few-micrometer tip

diameter, increasing the spatial resolution (Marg and Adams, 1967; Burns et al., 1974). This microwire method is still used in current neural recordings, as shown in Figure 2 (A).

The development of silicon etching technology has made it possible to produce microfabricated electrodes (Cheung, 2007). The Utah Electrode Array (Figure 2 (B)) is a three-dimensional electrode array with 100 needle-like silicon probes, which are micromachined from a block of silicon. The tip of each probe is coated with platinum, and the array is insulated with polyimide. (Campbell et al., 1991).
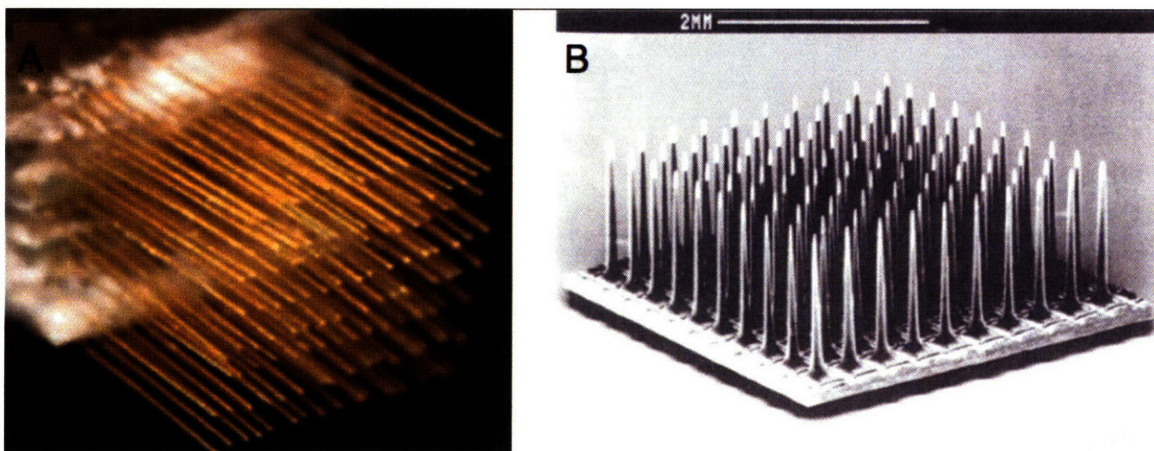
Figure 2. (A) Microwire multielectrode array (from Nicolelis et al., 2003) - an array of 128 stainless microwires is mounted on a printed circuit board. Each wire is approximately 50 µm in diameter and coated with Teflon except for the recording tip. (B) Utah Electrode Array (from Nordhausen et al., 1996) – 100 silicon electrodes insulated with polyimide.

Once these arrays are implanted in the brain, their structural supports are anchored to the skull. However, the brain moves relative to the skull due to the subarchnoid space. When the brain moves, the large mismatch in stiffness between "hard" electrodes and "soft" brain causes shear-induced inflammation at the implant site. This inflammation leads to the formation of a glial scar, limiting the long-term recording by electrically and mechanically isolating electrodes from neurons (Cheung, 2007).

Silicon photolithographic processing has improved electrode fabrication technology, providing precise control over electrode size, shape, texture, and spacing. As a result,

multiple recording sites can be placed at variable heights on an electrode probe (Figure 3 (A), (B)) (Vetter et al., 2004). This probe is called a Michigan probe, and Figure 3 (C) shows how it is implanted in the brain. The complete assembly includes the Michigan probe, a connector, and a flexible ribbon cable that connects the probe and the connector (Figure 3 (D)). Even though the connector is anchored on the skull, the probe is "floating" in the brain. The flexibility of the cable compensates for brain movement and reduces the chance of inflammation. However, small-scale motion still occurs between the electrode and the neuron, eliciting a host response that limits chronic recording.
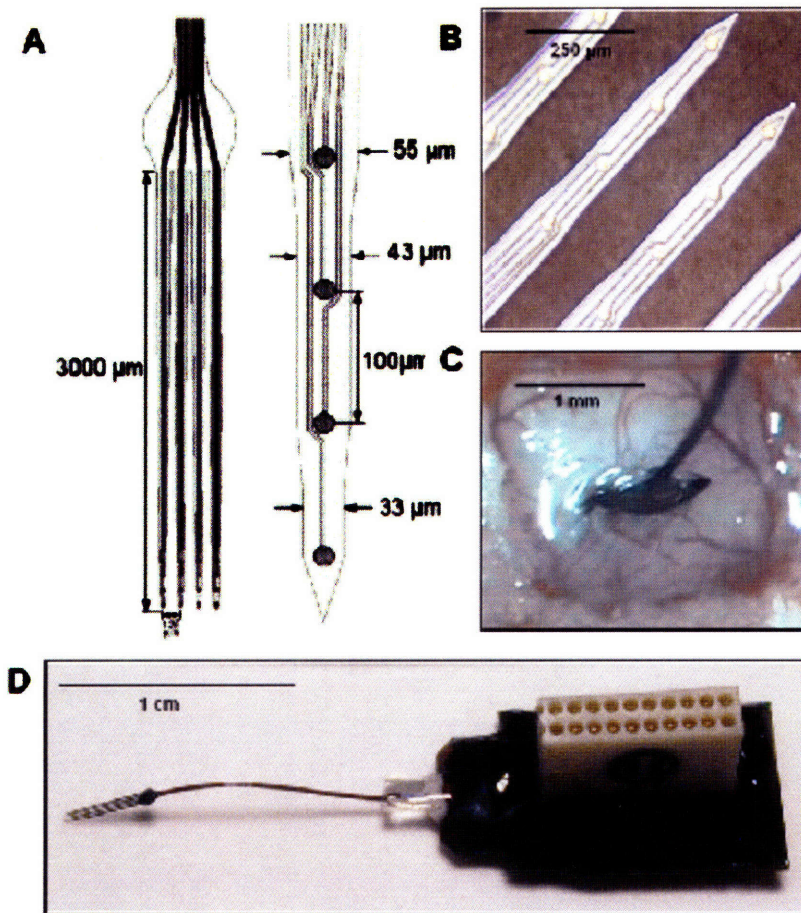

Figure 3. The Michigan probe with a flexible ribbon cable (from Vetter et al., 2004).

1.3 Conducting Polymers

Conducting polymers are novel materials that have high electrical conductivity, low stiffness, and promising biocompatibility. Some conducting polymers have been deposited on the recording sites of neural electrodes (Cui et al., 2001; 2003). The resulting rough morphology lowered the impedance of the electrode, improving the recording quality. In addition, biological factors such as cell adherence peptides and neurotrophins were incorporated into these conducting polymers to enhance cell-electrode interactions.

Microwires from these conducting polymers are an ideal candidate to replace metals in future neural electrodes. The Young's modulus of the polymers is approximately two orders of magnitude less than that of silicon or the metals typically used for neural recordings (Madden, 2002). Therefore, the flexibility of conducting polymers has the potential to improve long-term recording quality by decreasing the stiffness mismatch between the electrode and brain tissue.

1.4 Scope of Thesis

In this research, rather than merely coating a metal or silicon electrode, I attempted to record cortical activities with a microwire made entirely of Polypyrrole (PPy), a widely used conducting polymer in neural applications. This thesis demonstrates that it is possible to record cortical activities from a rodent brain with a conducting polymer microwire electrode. Chapter 2 presents and discusses the fabrication method for the electrode. Chapter 3 analyzes impedance of the PPy electrodes in saline under different voltage sweeping conditions. Chapter 4 provides cortical recording data and identifies action potentials. Chapter 5 provides conclusions and future research directions.

Chapter 2.   Conducting Polymer Electrodes

Conducting polymers are novel materials that have electrical properties similar to metals but mechanical, chemical, and manufacturing properties similar to conventional polymers (Heeger, 2002). This chapter provides background information about conducting polymers, focusing on PPy. In addition, the fabrication method of PPy electrodes is presented and discussed.

2.1   Background

The discovery of conducting polymers dates back to 1862 when Letheby first reported the anodic oxidation of aniline (Letheby, 1862). However, little was understood at that time, so the discovery was essentially lost. Conductive polymers were not recognized until 1977 when Shirakawa et al. synthesized halogen doped polyacetylene (10^3 S/m). Since then, over 25 conducting polymers have been reported with the commonality that they have a conjugated structure of alternating carbon-carbon double bonds (Skotheim, 1986).

In fact, undoped conducting polymers are semiconductors characterized by a band gap. With the addition of dopants to the polymer by oxidation or reduction of the conjugated π-molecular orbital backbone, conducting polymers can be highly conductive (Ateh, 2006).

Figure 4 shows the chemical structure of common conducting polymers. The most commonly explored conducting polymers for biomedical applications are polypyrrole (PPy), polythiophene (PT), poly(3,4-ethylene dioxythiophene) (PEDOT), and polyaniline (PANI) because they exhibit good stability, conductivity, and ease of synthesis (Kundu and Giri, 1996; Hong and Marnick, 1992). The conductivity of these common polymers is listed in Table 1.
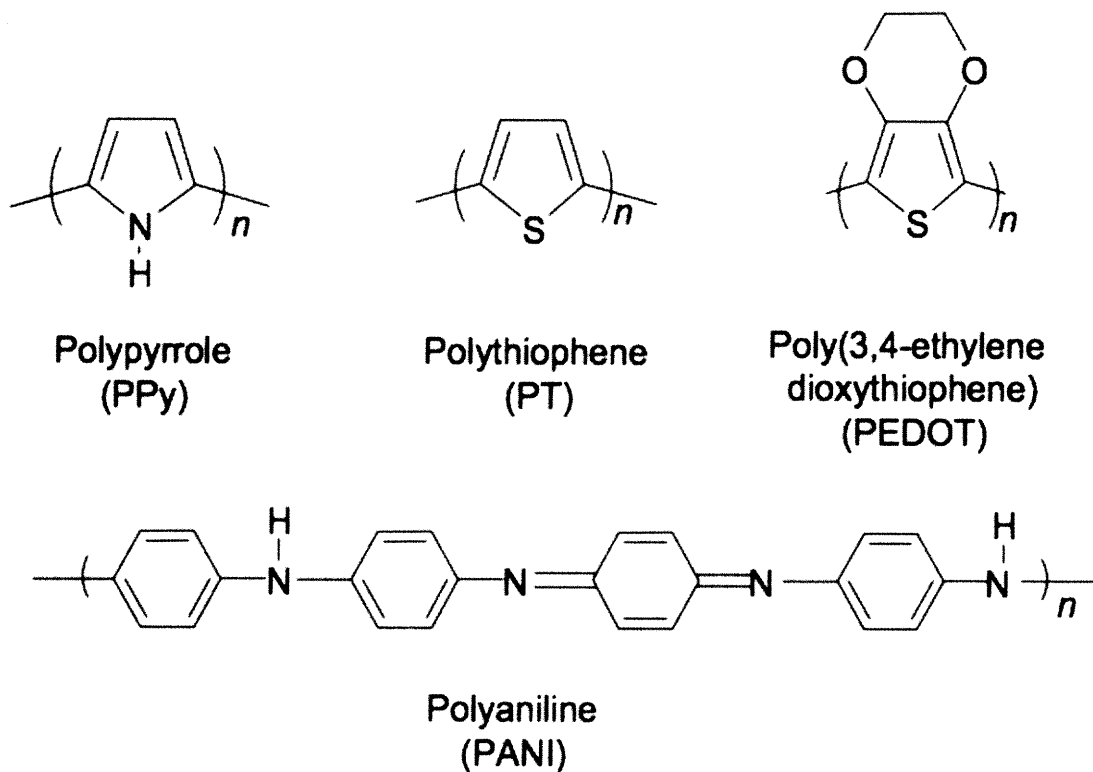
Figure 4. Common conducting polymers (from Guimard et al., 2007).

Conducting polymers have been used in diverse applications including actuators, transistors, strain gauges, chemical sensors, batteries, and photodiodes (Madden, 2003). With the discovery in the 1980s that these materials were compatible with many biological molecules, conducting polymers were researched for biomedical applications such as biosensors, tissue-engineering scaffolds, drug-delivery devices, bio-actuators, and neural probes. The major advantages for these applications include biocompatibility, the ability to entrap and controllably release biological molecules, the ability to transfer charge from a biochemical reaction, and the potential to easily alter physical properties (Guimard et al., 2007).

Table 1. Conductivity of common CPs (from Guimard et al., 2007).

Conducting polymer	PPy	PT	PEDOT	PANI
Conductivity (S/m)	4000-20000	1000-10000	100-17000	500

Most of initial studies exploring the applications of conducting polymers to neural electrodes were focused on PPy. PPy, doped with fibronectin and laminin fragments, was deposited on the recording site of a neural electrode (Cui et al., 2001). The resulting rough surface lowered the impedance of electrode, enhancing recording quality. In addition, preferential binding was reported for glial cells on films incorporating fibronectin fragments. This study showed that biomolecules that have cell adhesion functionality could be used in PPy-based electrodes to enhance cell-electrode interactions.

The biocompatibility of PPy in brain tissue has been investigated both in vitro and in vivo (George et al., 2005). PPy implants were produced under varying dopants and electrodeposition temperatures. Even though PPy was not incorporated with biomolecules, the response to all versions of PPy was at least comparable to that of Teflon implants in terms of macrophage activity, gliosis and neuronal integration.

Due to its excellent biocompatibility and conductivity, PPy was chosen as a representative conducting polymer for my research. The PPy microwire was prepared in the Bioinstrumentation lab at MIT, and the procedure is described in detail in the following section.

2.2 Fabrication of PPy microwires

PPy microwires were prepared as described in Ruddy, 2006.
PPy films were electropolymerized from a propylene carbonate solution containing tetraethylammonium hexafluorophosphate, and pyrrole. Electropolymerization was carried out galvanostatically in a two-electrode cell. Black PPy film, with an approximate thickness of 20 μm, was formed on a glassy carbon anode. PPy microwires were produced by mounting a PPy film perpendicular to the stage of a cryo-microtome and slicing it in 20 μm sections. Figure 5 shows a single PPy microwire with a cross section

of 20 μm × 20 μm. This microwire was then insulated with a vapor-deposited layer of Parylene 2-3 μm thick. In order to maintain an exposed length of polymer for an electrical contact later, approximately 10 mm of wire was placed between two glass cover slips and shielded from the Parylene deposition.
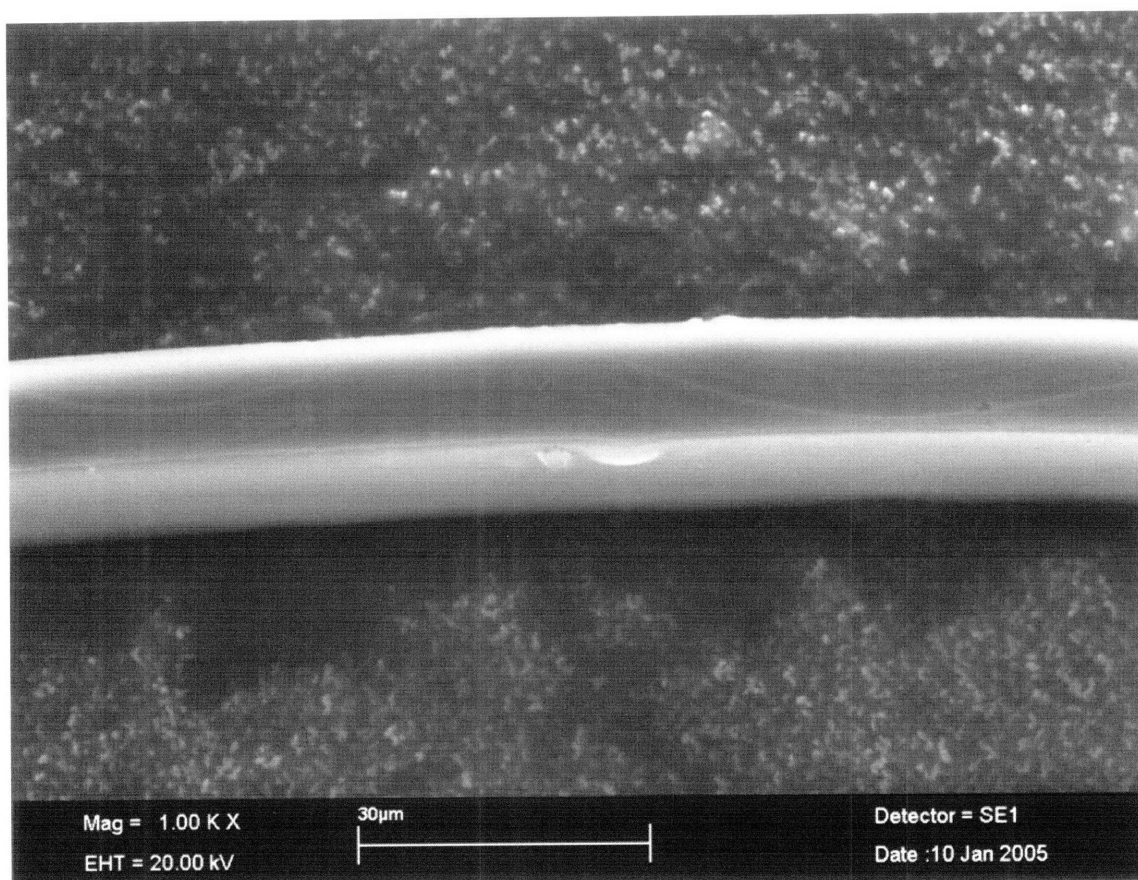

Figure 5. A length of 20 μm × 20 μm PPy wire prior to Parylene coating (from Ruddy, 2006).

2.3 Fabrication of PPy electrodes

The microwire fabrication process provides a wire with 40 mm insulated and 10 mm uninsulated segments. The uninsulated portion was inserted into a 10 mm length, 30 gauge hypodermic tube[1]. Crushing the tube with pliers provided a metal-polymer conductive interface. This hypodermic tube was then clamped into a male type miniature pin[2].

Figure 6 (A) shows a single microwire electrode connected to a copper wire. Closer views of the recording end and the connector end of the electrode are shown in (B) and (C), respectively. The electrode pin is mounted on a 2 mm diameter, 100 mm length glass tube[3] as shown in (A) and (C). This tube provides a long and rigid support to be held by a stereotaxic vertical manipulator. A 0.8 mm diameter capillary glass tube[4] of 15 mm length was attached to the near end of thick glass guide tube by epoxy as shown in (B). This capillary glass tube provided a rigid support to deliver the flexible polymer microwire into the cortex. The microwire was inserted into this thin glass tube until approximately 1 mm of polymer protruded beyond the tip of the tube. The electrode pin was then attached to a thick glass guide tube with tape (not shown). Cutting the protruded polymer at approximately 0.5 mm from its tip exposed a conductive recording site.

---

[1] Small Parts, Inc.
[2] Card Edge Connector from WPI
[3] Single Barrel Standard from WPI
[4] Drummond Scientific Company

(A)

Supporting Glass Tube

Centimeters

(B)

Capillary Glass Tube   Polypyrrole
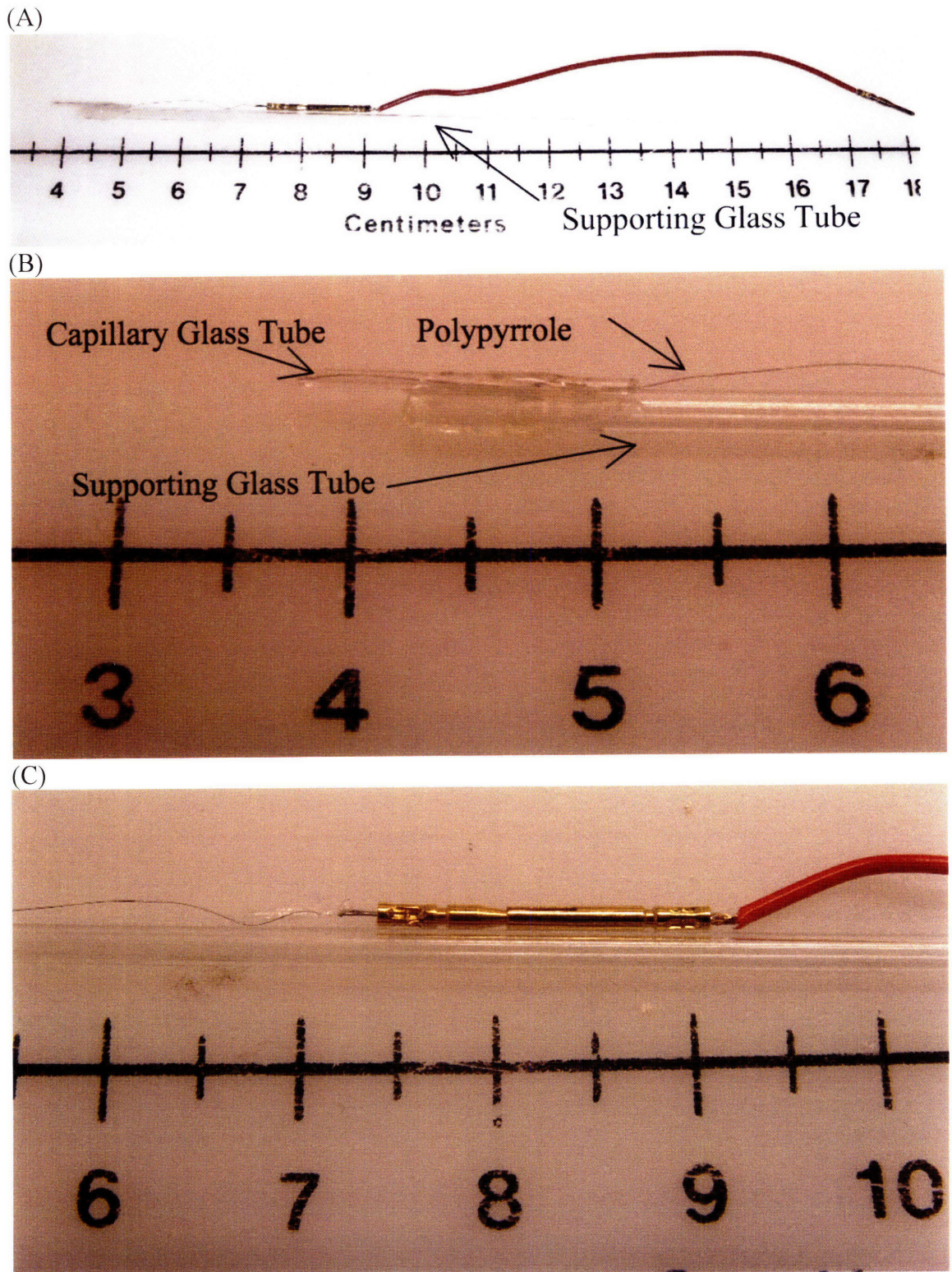
Supporting Glass Tube

(C)

Figure 6. A PPy microwire electrode. (A) Overall design, (B) closer view of a recording end, (C) closer view of a connector end. (All scales in cm).

16

2.4 Discussion

The conducting polymer electrodes share a similarity with the early metal-microwire electrodes. Both types of electrodes are produced in microwires with thin outer insulations, and the conductive sites are prepared by simply cutting off the tip of the microwires.

The original design for the polymer electrode was a harpoon design in which a PPy microwire was attached along a tungsten electrode; the recording tip was glued to the tip of the tungsten electrode using polyethylene glycol. The stiffness of the tungsten electrode delivered the PPy microwire into the cortex. Once the polyethylene glycol was completely dissolved in the brain, we expected to record activities. However, this approach was not successful over several trials on a rodent brain, and I suspected that the polyethylene glycol was not completely dissolved during an acute recording experiment. In Palmer's work, the dissolving time for polyethylene glycol was expected to be over 24 hours (Palmer, 1977). If the electrode was implanted over days, the coating must have completely dissolved. However, the cells around the tungsten electrode might have been damaged severely due to the micromotion of brain relative to the skull. Thus, this method was abandoned.

Using the capillary tube was a rather crude way to insert the PPy microwire in the brain because a diameter of 0.8 mm was large enough to cause severe damage during implantation. A thinner tube was considered, but inserting the PPy microwire in the tube was more challenging. In order to test the feasibility of the conducting polymer electrode, this capillary tube was acceptable. Since the tip of the microwire was left uncoated, the microwire was able to record cortical data once implanted.

Chapter 3.   Impedance Analysis of PPy Electrodes

This chapter evaluates the recording quality of polymer electrodes by measuring their impedance and monitoring their stability over time.

3.1 Electrode-Electrolyte Interface

In principle, a neural electrode is a transducer that converts the ionic currents flowing around the recording site to an electrical signal. These ionic currents represent the electrical states of nearby neurons (Kipke et al., 2004). Therefore, if action potentials occur, they affect the ionic currents in the extracellular space, and this change is measured through the electrode.

It is important to understand the electrode-electrolyte interface. Once the electrode is positioned in the brain, the interface reaches electrochemical equilibrium by either Faradaic reactions or capacitive redistribution of charges across the interface. At this equilibrium, a molecular layer of water coats the metal, acting as a dielectric between the metal and the electrolyte. Figure 7 (A) shows a schematic of this process for a metal electrode that has a negative surface charge. A layer of water molecules adheres to the electrode surface, and this layer is called an inner Helmholtz plane. Cations surrounded by water molecules form the outer Helmholtz plane. These two planes contribute to the capacitive nature of the interface (Kipke, Pellinen, and Rousche, 2004).

When an action potential occurs, the ions are transferred to the electrode either through direct exchange of ions or through redistribution of charges. The electrode-electrolyte system is often modeled with an equivalent circuit consisting of lumped resistances and capacitance as shown in Figure 7 (B). In this Randle's model, Re represents the ohmic resistance due to direct charge transfer across the interface; Ce represents the double

layer capacitance related to the Helmholtz planes. The resistance of the electrolyte between the interface and ground is represented by *Rsp*, which is also called the spreading resistance (Robinson, 1968). However, this model does not fully capture the true biological process, which deviates from ideal capacitors and resistors (Kipke, Pellinen, and Rousche, 2004).
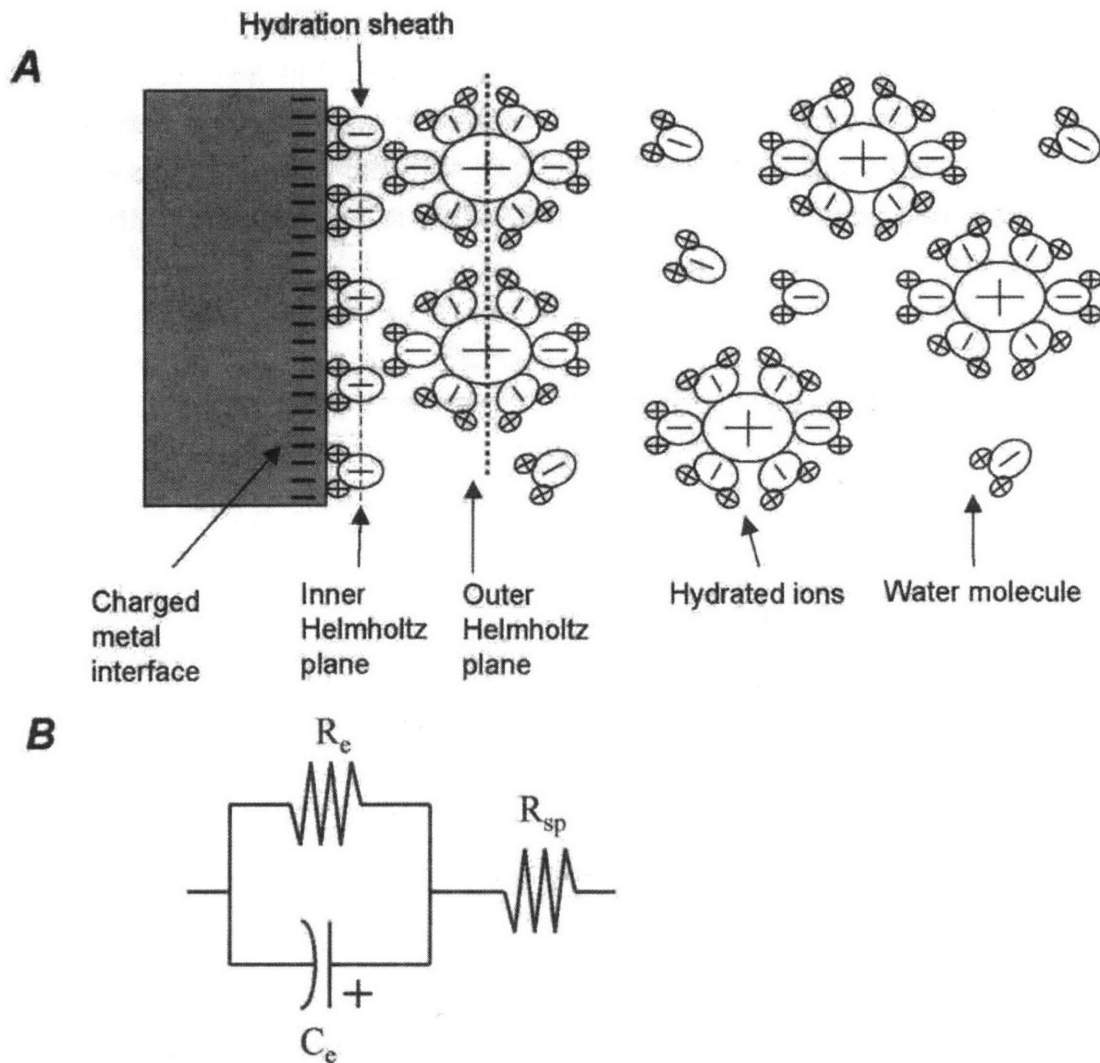

Figure 7. (A) Schematic of a metal electrode-electrolyte interface (from Kovac, 1998) (B) Equivalent Randle's circuit model of such interface.

Measuring electrode impedance provides quantitative values for model parameters. The impedance, $Z(j\omega)^5$, is the ratio of the AC voltage across the interface to the current through the interface,

$$Z(j\omega) = \frac{V(j\omega)}{I(j\omega)} = \mathrm{Re}(Z) + j\,\mathrm{Im}(Z). \tag{1}$$

With Randle's model parameters,

$$Z(j\omega) = R_{sp} + \frac{R_e}{1+(R_eC_e\omega)^2} - j\frac{R_e^2C_e\omega}{1+(R_eC_e\omega)^2}. \tag{2}$$

The magnitude refers to the absolute value of Z, and the phase refers to the angle between real and imaginary values as in

$$|Z| = \sqrt{(\mathrm{Re}(Z))^2 + (\mathrm{Im}(Z))^2}$$
$$\theta = \arctan\left(\frac{\mathrm{Im}(Z)}{\mathrm{Re}(Z)}\right). \tag{3}$$

Figure 8 illustrates the general shape of Randle's model with arbitrary parameters (Rsp=1 kΩ, Re=100kΩ, and Ce=10nF). When the frequency is close to 100 Hz, the magnitude is 20 kΩ with a phase of -2 degrees. As the frequency increases to 1 kHz, both the magnitude and the phase drop to 18 kΩ and -15 degrees. Beyond 10 kHz, the magnitude is flat at 10 kΩ, and the phase returns to zero degrees.

A pure resistor has a phase of zero degree, whereas a pure capacitor has a phase of -90 degrees. Therefore, by analyzing the phase plot, the nature of the interface can be determined. In addition, impedance at 1 kHz is usually a representative value used to determine the recording quality of electrodes because the duration of action potentials is usually 1 ms.

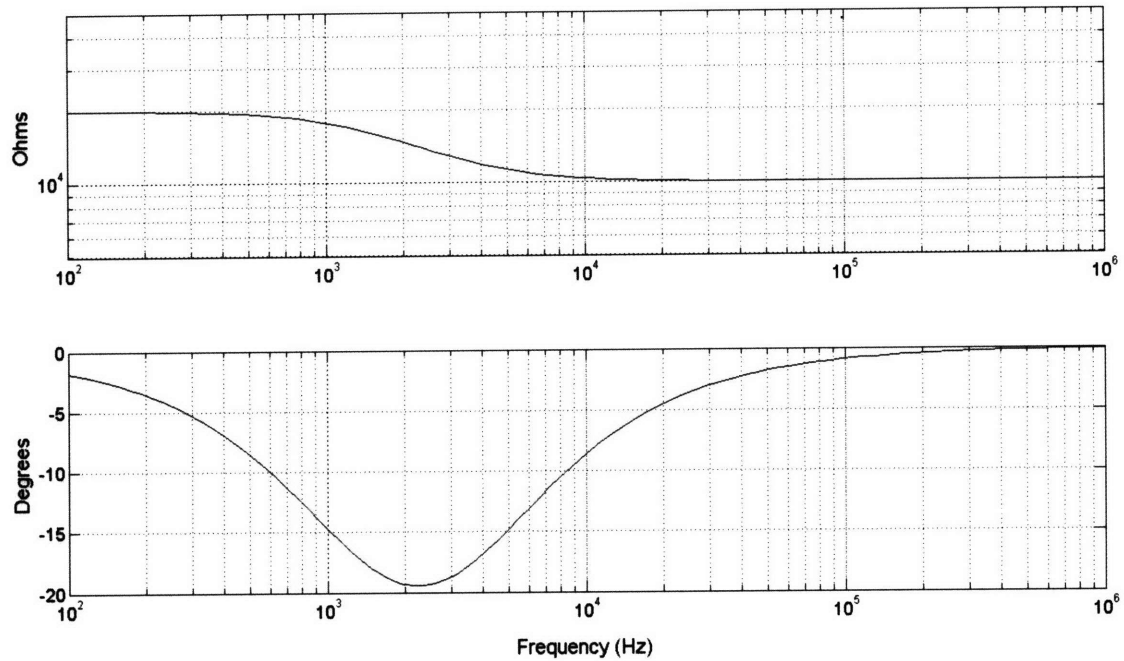[5] ω refers to the frequency of AC voltage, and $j = \sqrt{-1}$.

Figure 8. Bode plot of Randle's model.

The ability to record action potentials from neurons is dependent on a tradeoff between the geometric area of the recording site and its impedance. In other words, it is the tradeoff between "selectivity" and "sensitivity" (Kovac, 1998). As the recording site becomes smaller, it can isolate the action potential of a single neuron. However, the impedance of an electrode increases, adding noise to the neural signals (Kipke et al., 2004).

3.2 Impedance Measurement Setup

The impedances of the electrodes were measured with the HP 4194A Impedance/Gain-Phase Analyzer. Approximately 20 mm of polymer wire was immersed in physiological saline. The working electrode was the polymer microwire, and the counter electrode was a silver coated copper wire. An AC voltage of 20 mV peak-to-peak was applied with a frequency sweep from 100 Hz to 1MHz. Figure 9 shows the measurement setup.
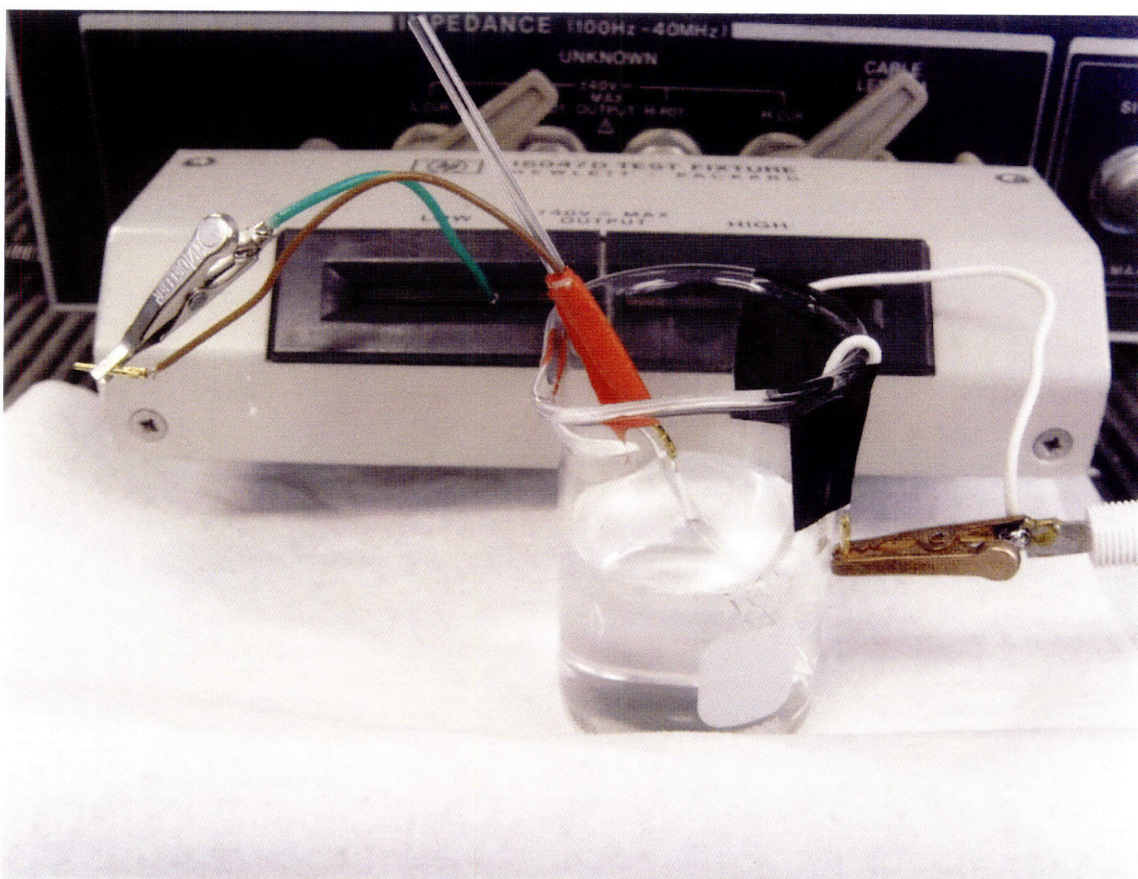

Figure 9. Impedance Measurement Setup. A white alligator clip is connected to a counter electrode, and a green alligator clip is connected to the electrode.
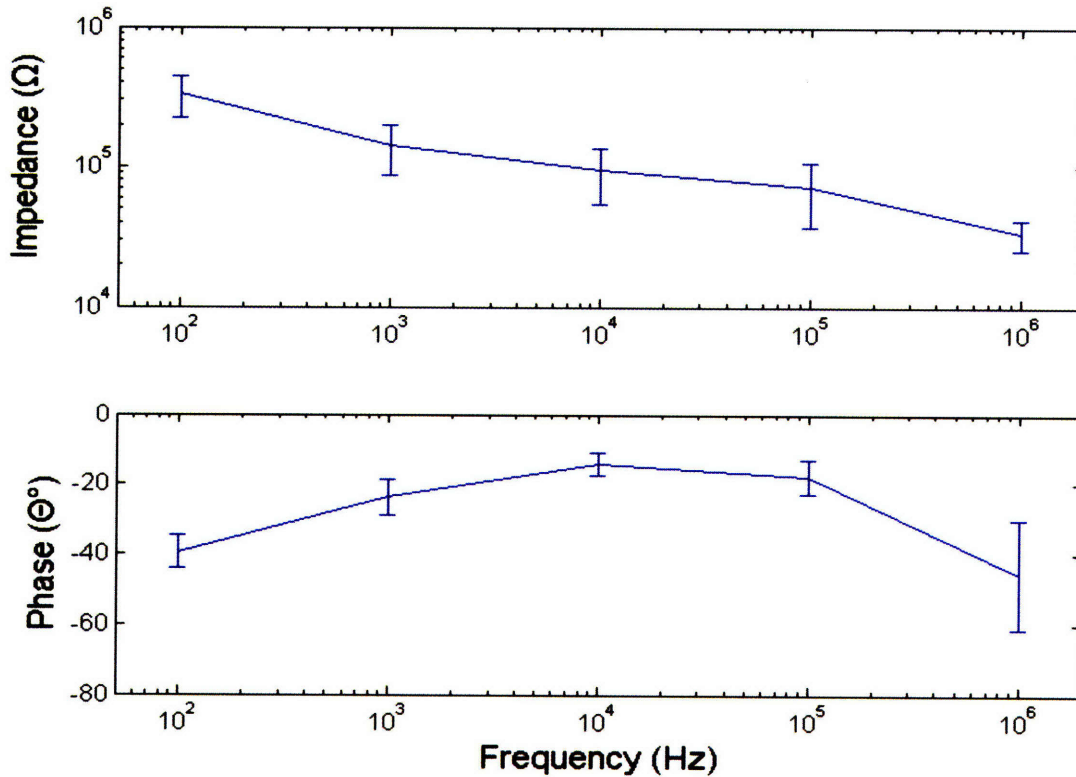
3.3 Results

3.3.1 Initial impedance

Figure 10. Impedance data of the PPy electrode in saline (mean +/- std, n=5).

Figure 10 shows the mean (+/- std) impedance of five polymer electrodes immersed in saline for approximately 1 minute. The magnitude decreases with increasing frequency. The phase is less than 45 degrees up to 100 kHz. At 1 kHz, impedance is 142 ± 55 kΩ with a phase of -24 ± 5.3 degrees. Compared to a metal electrode, for which the phase is closer to -90 degrees, the interface of the PPy electrode shows a more resistive nature. Considering the cross sectional area of 4×10^{-10} m^2, the impedance magnitude is in accordance with previous work with PPy-coated electrodes (Abidian and Martin, 2008).

## 3.3.2 Stability of impedance with a continuous voltage sweep

A continuous AC voltage sweep was applied to one PPy electrode while it was immersed in physiological saline. The amplitude was 10 mV, which is the minimum setting of the instrument. The impedance at 1 kHz over 125 hours is plotted in Figure 11 (A). Figure 11 (B) magnifies the first 20 hours of data.

The initial impedance is 150 kΩ with a phase of -25 degrees. Within the first two hours, the impedance increases to 1 MΩ, and the phase decreases to -60 degrees. After that, the impedance slowly decreases to 300 kΩ and starts to increase again beyond 1 MΩ. At the same time, the phase approaches zero degrees. This set of data shows that the interface becomes resistive, and impedance is continuously increasing as the phase approaches zero degrees.
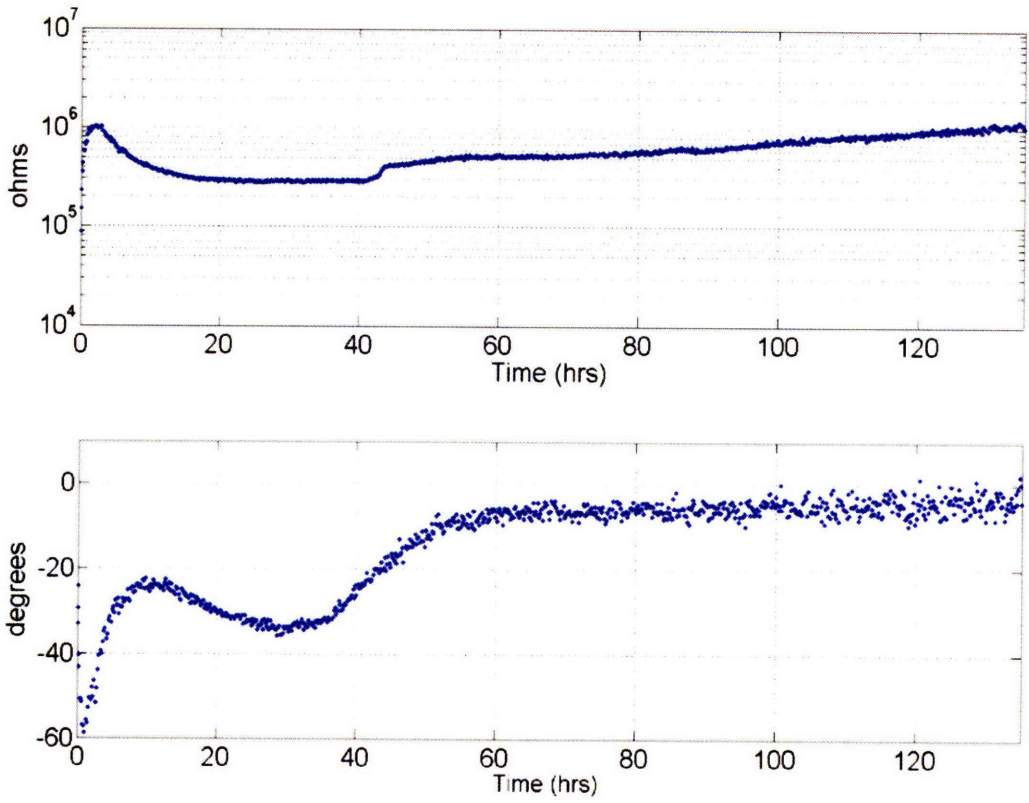
(A)
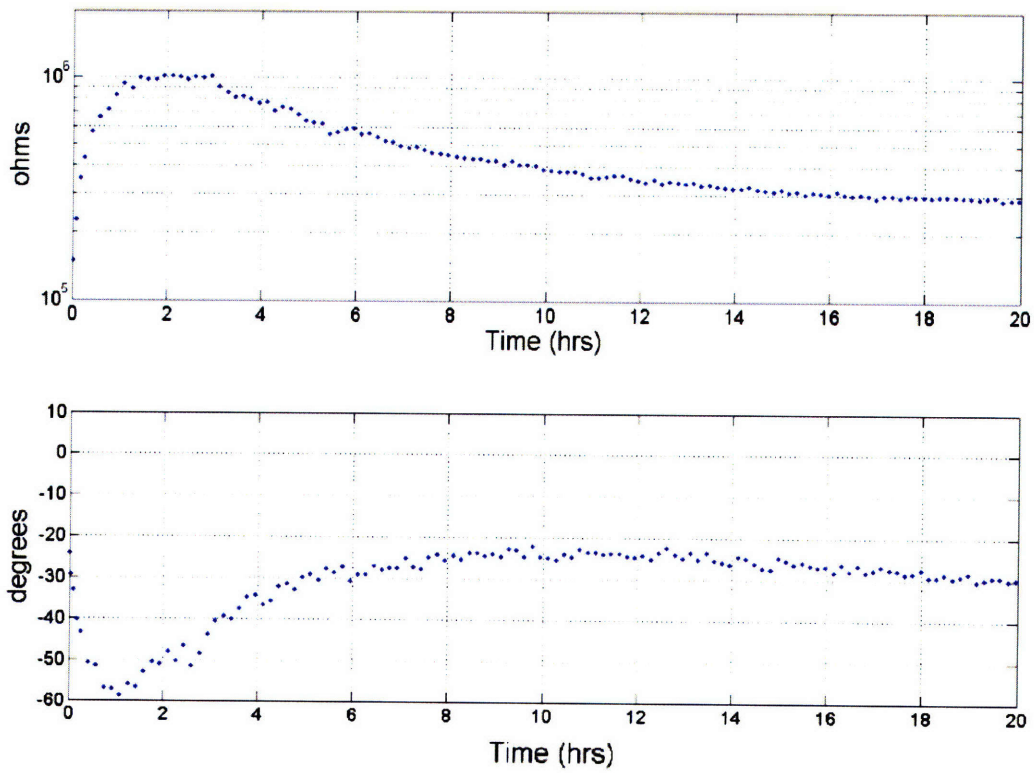
(B)

Figure 11. (A) Impedance at 1 kHz for 120 hrs (B) Closer view of the first 20 hours of data.

The bode plots of significant time points from Figure 11 are plotted in Figure 12. The shape of each plot is distinctly different from one another, suggesting that a dynamic change is occurring at the electrode interface. In addition, a simple Randle's model is not sufficient to capture this change over time. The magnitude of the impedance always decreases as frequency increases. However, the phase near 1kHz decreases for the first hour and then approaches zero degrees afterwards. The last data set is similar to the first-order RC model.
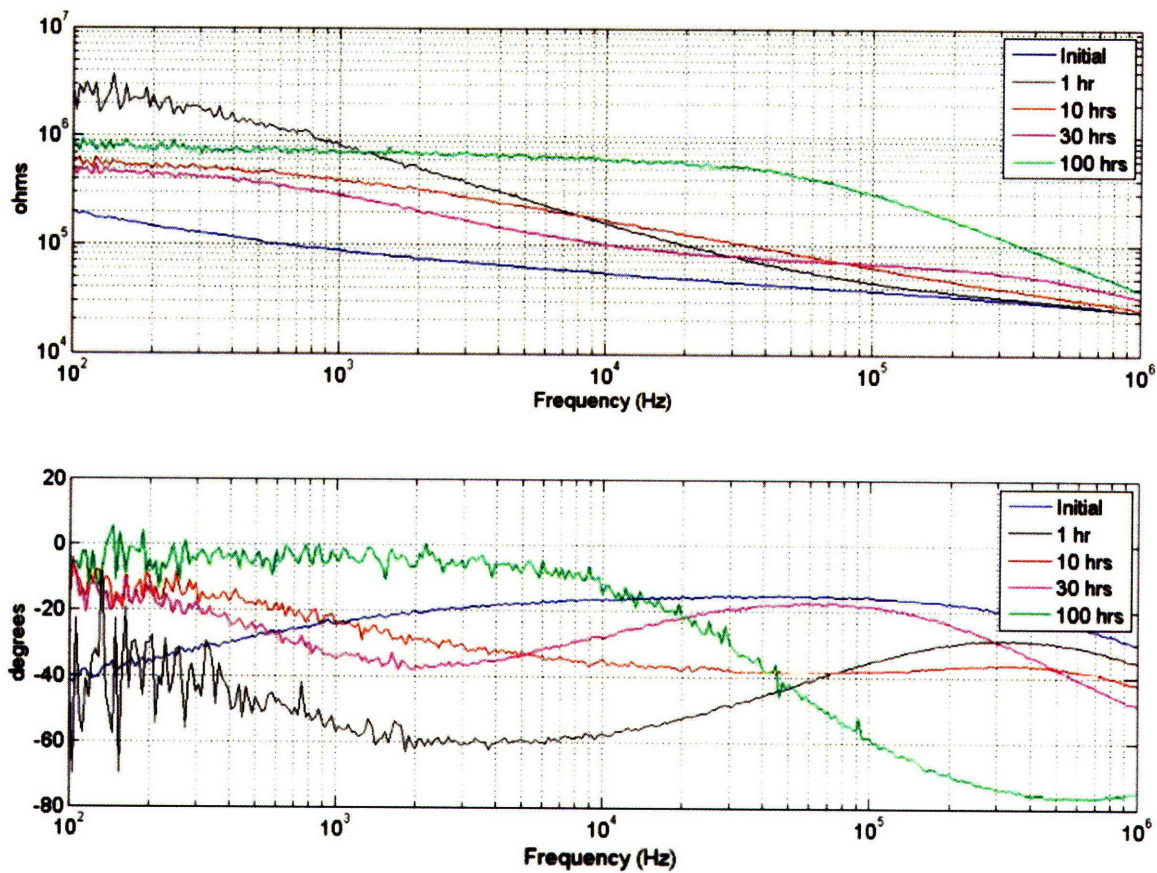

Figure 12. Bode plots of impedance at five time points – Initial, 1 hr, 10 hrs, 30 hrs, and 100 hrs.

3.3.3 Stability of impedance for a repetitively used electrode with a continuous voltage sweep

The PPy electrode used in Figure 11 was excited by a continuous voltage sweep for an additional two runs. The tip of the PPy microwire was cut off with a razor blade for each run. Impedance at 1 kHz of this second run is plotted Figure 13 (A); the third run in Figure 13 (B). It is interesting to see that cutting the tip results in a low impedance interface. One notable difference for the second run in comparison to the first one is that a significant increase in impedance was measured after 30 hours. In the third run, this increase was observed in 12 hours.

One possible cause of losing conductivity is due to diffusion of dopants. As the dopants in the interface diffuse out to the electrolyte, the electrode becomes non-conductive; therefore, the impedance increases. However, the diffusion of dopants is not sufficient to explain why impedance increases faster with a repetitive sweep. Since cutting off the tip produces a comparable interface each time (impedance of approximately 100 kΩ), if the impedance increase were caused only by diffusion, all the runs should be identical. Other possible causes for the discrepancy of the runs are under investigation.
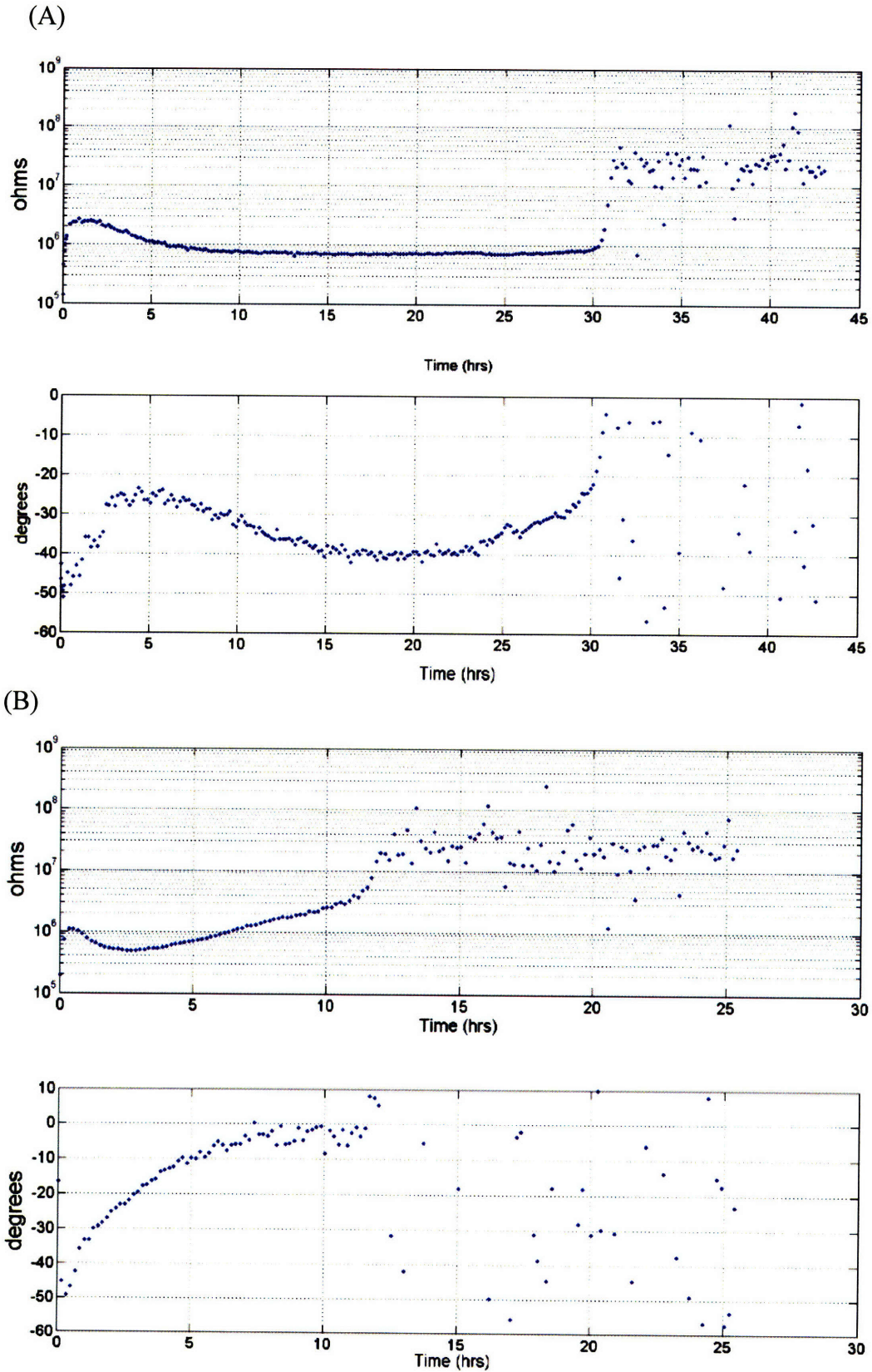
(A)

(B)

Figure 13. Impedance at 1 kHz from the second run (A), and the third run (B). The first run data are shown in Figure 11.

28

3.3.4 Stability of impedance without a continuous voltage sweep

The amplitude of action potentials recorded in extracellular space is usually hundreds of microvolts. Even though 10 mV was the minimum voltage setting for the instrument, this amplitude is approximately 2 orders of magnitude higher than the amplitude of action potentials. By not applying a voltage sweep, the electrode is maintained at a 0 mV, which could simulate the extracellular space better. Figure 14 shows the impedance change of the electrode in saline without any connections to the instrument. Compared to the previous plots, the impedance still increases but at a much slower rate; the impedance is less than 600 kΩ even after 370 hours.
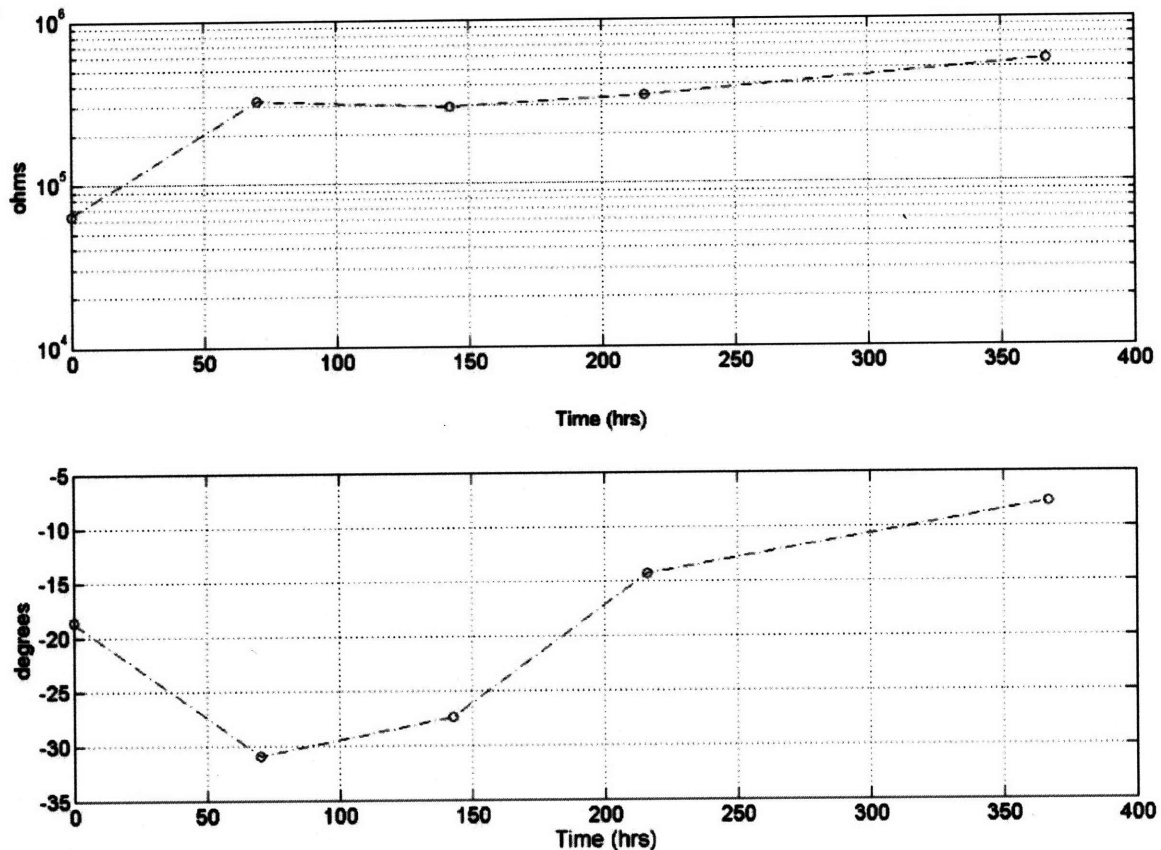

Figure 14. Impedance at 1kHz without a continuous voltage sweep. Even after 370 hours, impedance is less than 600 kΩ.

Bode plots at various time points for this PPy electrode are presented in Figure 15. The dynamics of the bode plots are similar to those of the 10 mV data set except that the change happens at a slower rate. The Bode plot at 370 hrs is again close to the first-order RC model because of the diffusion of dopants.
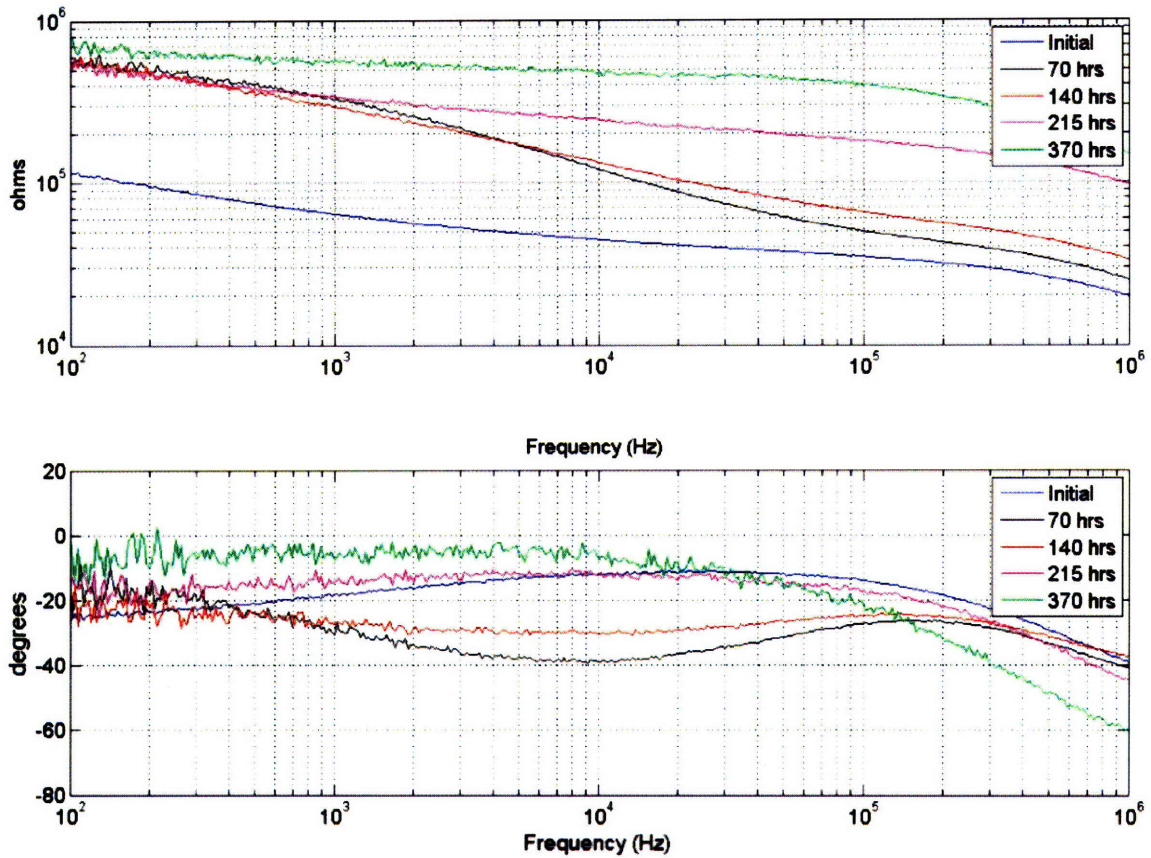

Figure 15. Bode Plot of PPy Electrode without continuous sweep at 0 hr, 70 hrs, 140 hrs, 215 hrs and 370 hrs.

3.3.5 Modeling

Modeling the interface with one equivalent circuit was challenging and beyond the scope of this thesis. The time change of Bode plots empirically shows that at least three distinctive models emerge over time (at initial, 70 hrs, and 370hrs). The simplest shape is the 370-hour data. It is well fitted with Randle's model, and the corresponding parameters are in reasonable agreement with the literature.
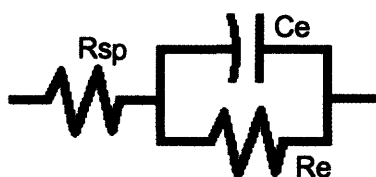

Figure 16. Randle's model.

Experimental data was fitted using the nonlinear least squares method in the ZSimWin[6] software. The calculated values were Rsp=65 kΩ, Re=473 kΩ and Ce=1.55 pF. The order of the value for Rsp is in accordance with the literature (Robinson, 1968), where

$$Rsp = \frac{\rho}{2\pi d}. \tag{4}$$

In Equation (4), ρ is resistivity, which is 0.725 Ω m for saline. The chi-square value is 0.03, which indicates the goodness of fit between the model and the data.
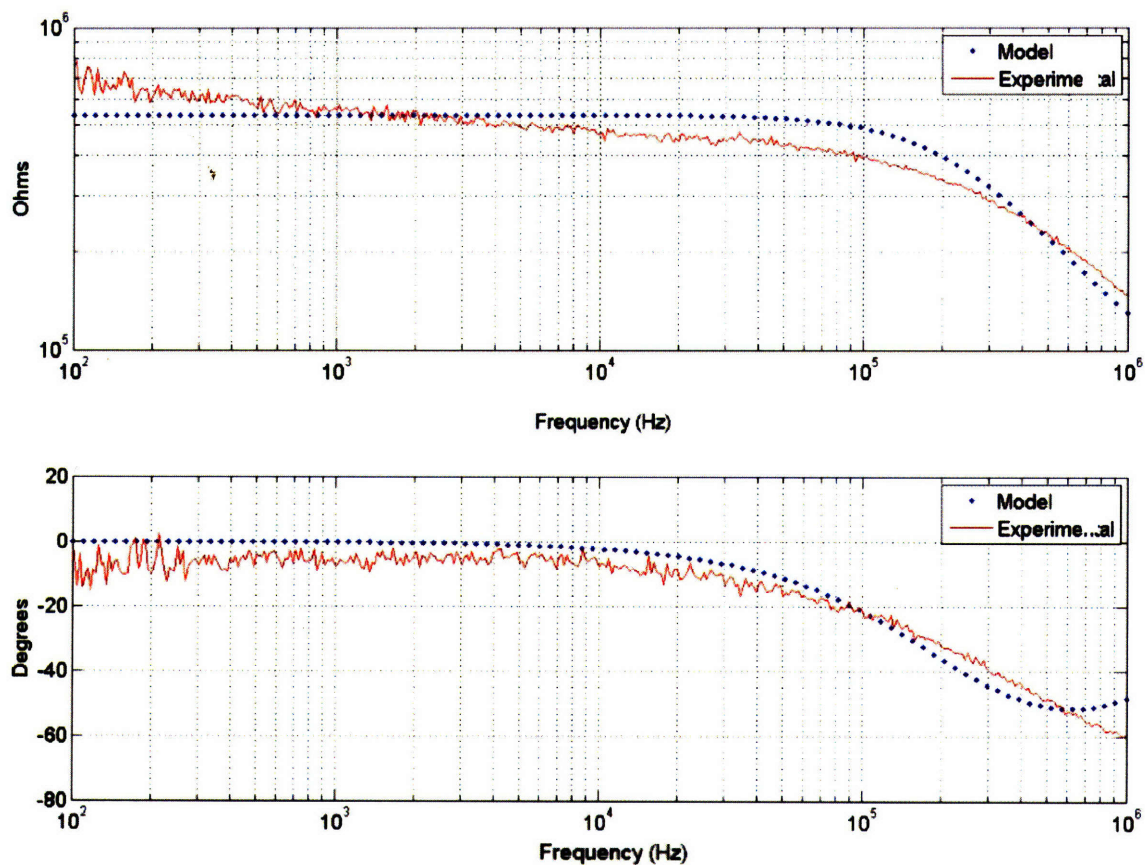
---

[6] www.echemsw.com

Figure 17. Modeling of 370-hour data set from Figure 15.

3.4 Summary

An increase in impedance of the PPy electrode was observed when a 10 mV AC voltage sweep was continuously applied. The tip of the electrode was cut off, and two additional runs of voltage sweeps were applied to the electrode. Even though the initial impedance was as low as the previous run, the impedance increased over time at a faster rate. Measuring the impedance without a continuous sweep also showed the increase in the impedance but at a slower rate. The shape of bode plots, both with and without continuous sweeps, shows similar dynamics at the interface. The loss of conductivity can be attributed to the diffusion of dopants in the saline.

Chapter 4.   Cortical Recording

Conducting polymer electrodes were implanted in a rodent brain. Cortical activities are usually recorded approximately 2 mm below the surface of the brain. The surgery procedure and cortical activities are presented in this chapter.

4.1   Surgical procedure

The surgery procedures were approved by the Massachusetts Institute of Technology Committee on Animal Care.   A 430-gram Sprague-Dawley rat was anesthetized with Xylazine-Ketamine. The animal was laid supine and secured in a stereotaxic device using head posts and a mouth clamp (Figure 19). A craniotomy of 5 mm in radius was created 1 mm lateral of bregma in the left hemisphere. An electrode manipulator held the supporting glass guide tube and lowered the electrode into the cortex. The electrode was lowered approximately 2 mm below the cortical surface.
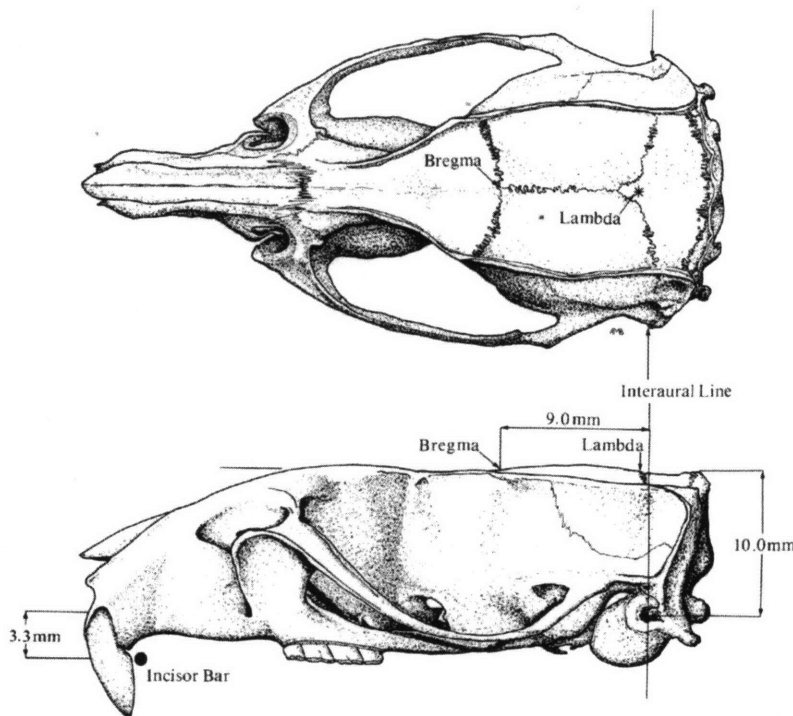

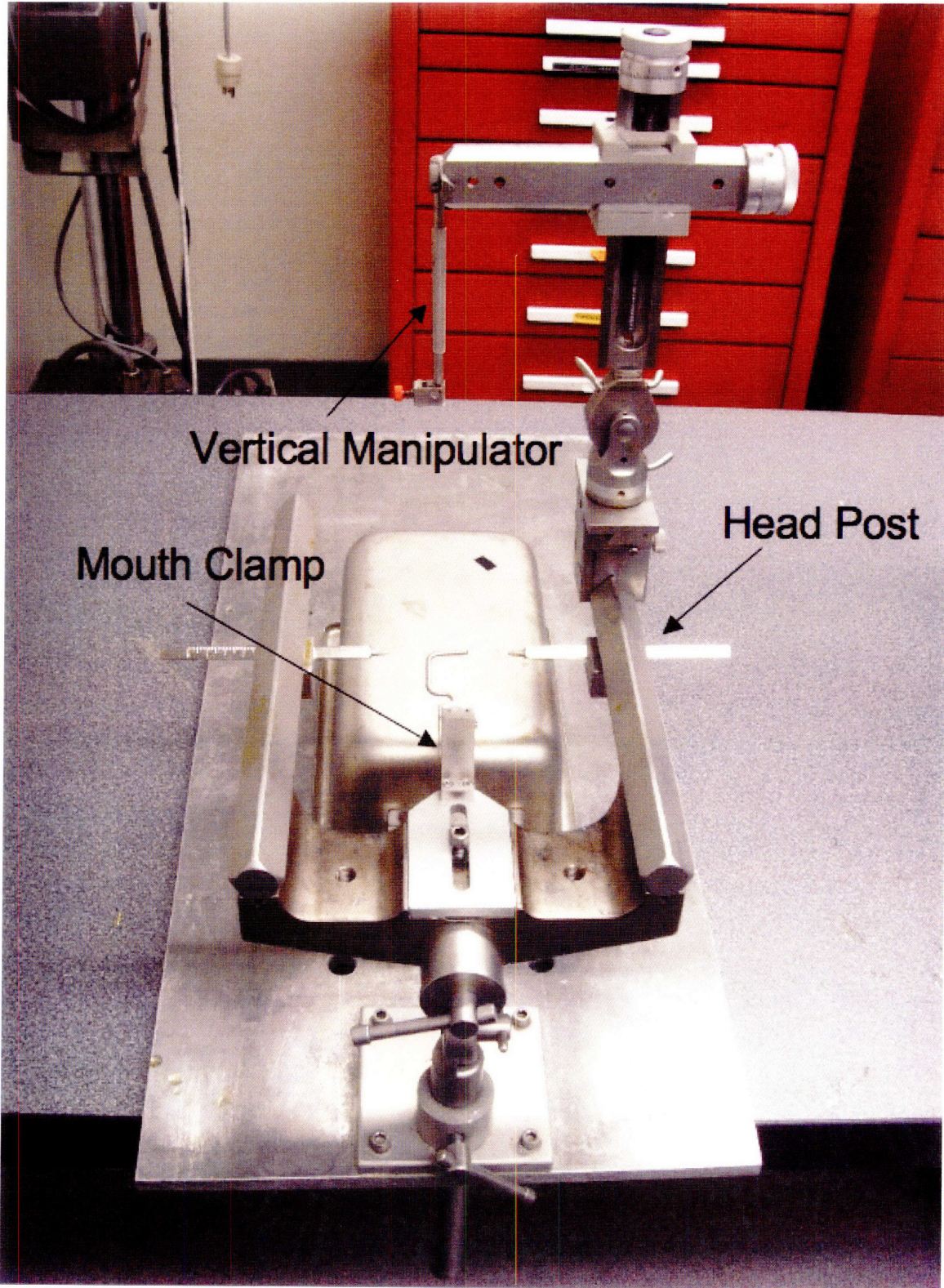Figure 18. Rodent Skull Diagram (from Paxinos and Watson, 1984).

Figure 19. A stereotaxic device including head posts, a mouth clamp, and vertical manipulator to hold an electrode.

4.2 Recording setup

The signals were amplified and bandpass-filtered (300 Hz to 10 kHz) by a CyberAmp 380[7]. The sampling rate was 20 kHz, and a faradaic shield enclosed the animal to minimize external electrical noise.

4.3 Results

4.3.1 Sample set of cortical data

Action potentials were recorded in the left hemisphere (1 mm lateral to bregma, 2 mm deep) for 1 hour and 30 minutes. Figure 20 shows sample raw recording data for 20 seconds. The RMS noise is approximately 20 µV, whereas the average spike is 140 µV peak-to-peak. With a good signal-to-noise ratio (SNR), action potentials are clearly observed in the plot.

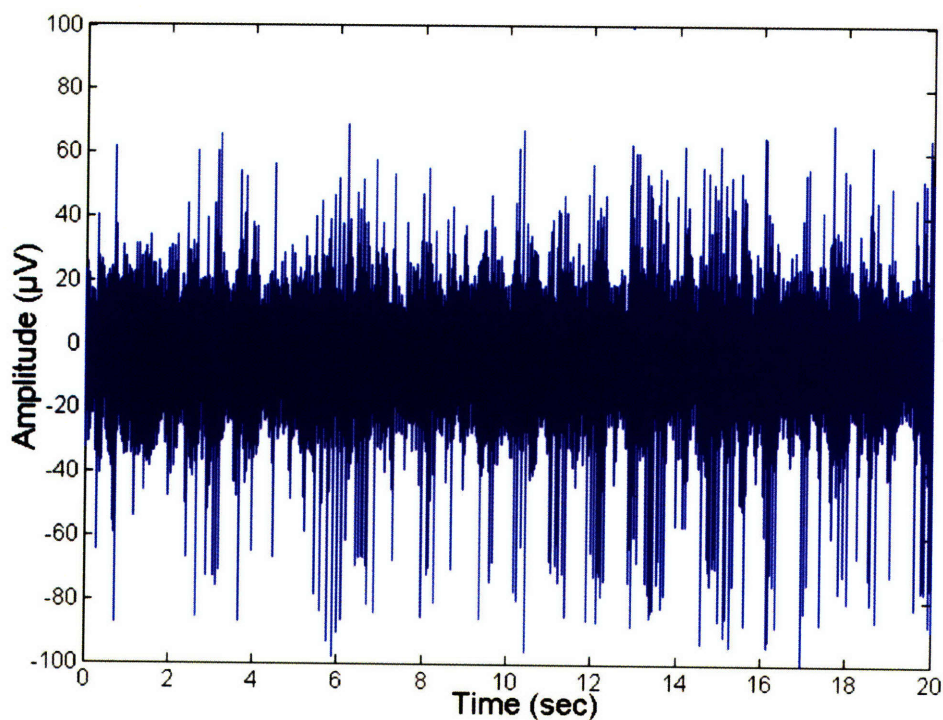Figure 20. Raw cortical activities with a PPy microwire electrode.
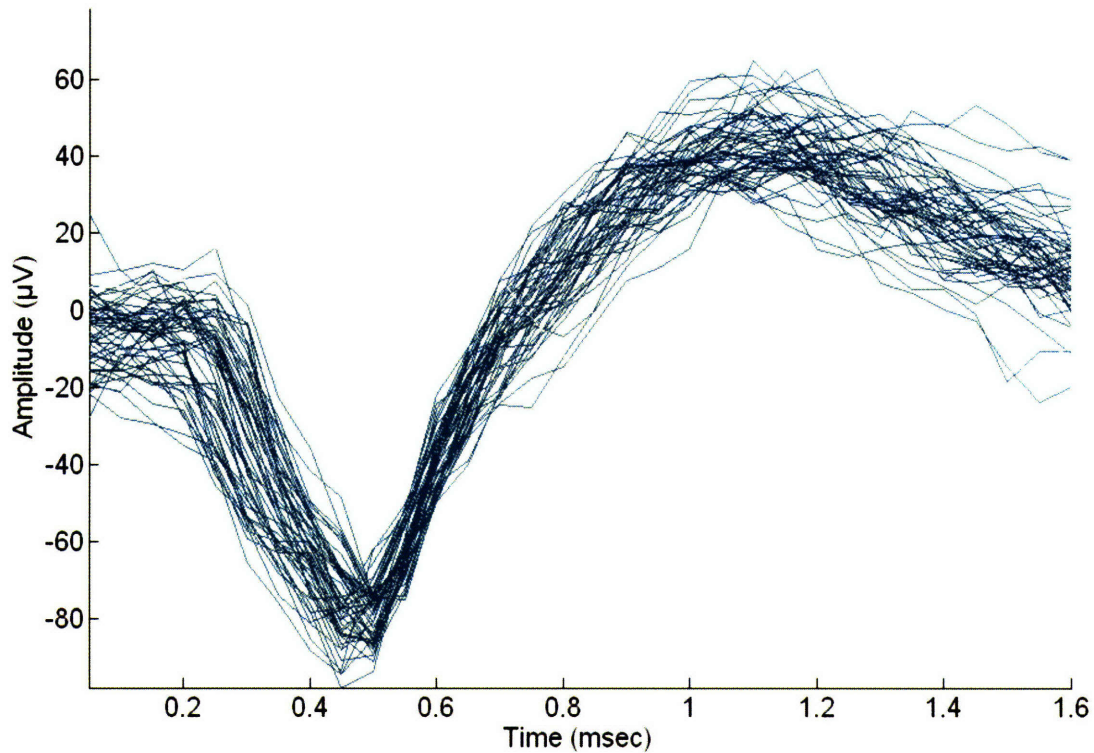

4.3.2 Action Potentials

Figure 21. Overlaid action potentials from the raw data.

The spikes in Figure 20 were identified using Mclust[8] and were overlaid within a time window of 1.6 msec. The repetitive waveforms confirm that the signals were indeed action potentials from a neuron.

---

[8] www.stat.washington.edu/mclust

Chapter 5.   Conclusions and Future Directions

A polypyrrole (PPy) microwire electrode was fabricated and implanted in a rodent brain to record cortical neural activities. The impedance analysis indicated that the recording site interface had a resistive nature. However, the conductivity of the electrode decreased over time due to the diffusion of dopants. The polymer electrode recordings had a good SNR to observe clear action potentials.

The success of cortical recording proves the feasibility of conducting polymer electrodes and motivates the next stages of development. Since the current PPy has the problem of losing conductivity over time, a variety of dopants should be deposited on the PPy in order to find the ones that provide consistent and high conductivity in saline. Possible lists of dopants are Cl⁻, dodecyl benzene sulfonate, ClO_4, poly styrene sulfonate, p-toluene sufonate, poly vinylsulfonic acid, and camphorsulfonic acid. In addition, the tip of the PPy electrode will be functionalized with fibronectin or laminin fragments as shown in the work of Cui et al. to enhance cell-electrode interactions and preferably to bind with neurons chronically (Cui et al., 2001).

The most challenging problem of this project is how to deliver the flexible microwires into the brain. A possible method is to coat them with materials that are initially rigid to penetrate the pia mater but become either biodegradable or flexible in response to the chemical environment within the brain. A polymer that has the ability to alter the stiffness in physiological solutions was recently reported (Capadona et al., 2008). Even though the biocompatibility of this material was not evaluated, it has the promising property for further investigations.

In order to record from multiple neurons, an array of the polymer electrodes should be considered. The array design can be similar to the current metal multi-electrode arrays where tens of electrodes are mounted on a substrate and electrically isolated from one

another. The substrate can be made of a sheet of a polymer so that the flexibility of the substrate compensates the micromotion between brain tissue and the electrodes.

References

Abidian, M.R., and Martin, D.C., (2008) *Experimental and theoretical characterization of implanatable neural microelectrodes modified with conducting polymer nanotubes.* Biomaterials 29: pp. 1273-1283.

Ateh, D.D., Navsaria, H.A., and Vadgama, P., (2006) *Polypyrrole-based conducting polymers and interactions with biological tissues.* J R. Soc. Interface 3: pp 741- 752.

Bear, M.F., Connors, B.W., and Paradiso, M.A., (2007) *Neuroscience exploring the brain*, 3rd ed. Baltimore: Lippincott Williams & Wilkins.

Burns, B.D., Stean, J.P.B., and Webb, A.C., (1974) *Recording for several days from single cortical neurons in completely unrestrained cats.* Electroenceph Clin Nuerophysiol 35: pp. 314-318.

Capadona, J.R., Shanmuganathan, K., Tyler, D.J., Rowan, S.J., and Weder, C., (2008) *Stimuli-responsive polymer nanocomposites inspired by the sea cucumber dermis.* Science 319: pp. 1370-1374.

Cheung, K.C., (2007) *Implantable microscale neural interfaces.* Biomedical Microdevices 9: pp. 923-938.

Cui, X., Lee, V.A., Raphael, Y., Wiler, J.A., Hetke, J.F., Anderson, D.J., and Martin, D.C., (2001) *Surface modification of neural recording electrodes with conducting polymer/biomolecule blends.* J Biomedical Material Research 56(2): pp. 261-72.

Cui, X., Wiler, J., Dzaman, M., Altschuler, R.A., and Martin D.C., (2003) *In vivo studies of polypyrrole/peptide coated neural probes.* Biomaterials 24: pp. 777-787.

George, P.M., Lyckman, A.W., LaVan, D.A., Hegde, A., Leung, Y., Avasare, R., Testa, C., Alexander, P.M., Langer, R., and Sur, M., (2005) *Fabrication and biocompatibility of polypyrrole implants suitable for neural prosthetics.* Biomaterials 26: pp.3511-3519.

Guimard, N.K, Gomez, N., Schmidt, C.E., (2007) *Conducting polymers in biomedical engineering.* Progress in Polymer Science 32: pp. 876-921.

Heeger, A.J., (2002) *Semiconducting and metallic polymers: the fourth generation of polymeric materials.* Synthetic Metals. 125: pp. 23-42.

Hong, S.Y., and Marnick, D.S., (1992) *Understanding the conformational stability and electronic structures of modified polymers based on polythiophene.* Macromolecules pp. 4652-2657.

Kipke, D.R., Pellinen, D.S., and Rousche, P.J., (2004) *CNS recording electrodes and techniques*. In: Neuroprosthetics Theory and Practice, 1st ed., edited by Horch, K.W. and Dhillon, G.S., Singapore: World Scientific Publishing Co. Pte. Ltd.

Kovacs, G.T.A., (1998) *Micromachined Transducers Sourcebook*. Boston: McGraw-Hill Publishing, p. 911.

Kundu, K., and Giri, D., (1996) *Evolution of the electronic structure of cyclic polythiophene upon bipolaron doping*. Am Inst Phys 105: pp. 11075-11080.

Letheby, H., (1862) *On the production of a blue substance by the electrolysis of sulphate of aniline*. J of Chemical Society 15: pp. 161-163.

Madden, J., (2002) *Conducting polymer actuators*. Ph.D. Thesis, MIT.

Madden, P., (2003) *Development and modeling of conducting polymer actuators and the fabrication of a conducting polymer based feedback loop*. Ph.D. Thesis, MIT

Marg, E. and Adams, J.E., (1967) *Indwelling multiple micro-electrodes in the brain*. Electroenceph Clin Nuerophysiol 23: pp. 277-280.

Nicolelis, M.A.L. et al., (2003) *Chronic, multisite, multielectrode recordings in macaque monkeys*. Proceedings of the National Academy of Sciences 100(19): pp. 11041-11046.

Nordhausen, C.T., Maynard, E.M., and Normann, R.A., (1996) *Single unit recording capabilities of a 100 microelectrode array*. Brain Research 726: pp. 129-140.

Paxinos, G. and Watson, C., (1986) *The rat brain in stereotaxic coordinates*, 2nd ed, San Diego: Academic Press INC.

Palmer, C., (1977) *A microwire technique for recording single neurons in unrestrained animals*. Brain Research Bulletin 3: pp. 285-289.

Robinson, D.A., (1968) *The electrical properties of metal microelectrode*. Proc. IEEE 56(6): 1065-1071.

Ruddy, B.P., (2006) *Conducting polymer wires for intravascular neural recording*. Master's Thesis, MIT.

Shirakawa, H., Louis, E.J., MacDiarmid, A.G., Chiang, C.K., and Heeger, A.J., (1977) *Synthesis of electrically conducting organic polmers: halogen derivatives of polyacetylene, (CH)$_x$*. J Chem Soc Chem Communi pp. 578-580.

Skotheim, T.A., (1986) *Handbook of conducting polymers*. Vol 1-2. New York, NY: Marel Dekker.

Strumwasser, F., (1958) *Long-term recording from single neurons in brain of unrestrained mammals*, Science 127: pp. 469–470.

Tolias, A.S., Ecker, A.S., Siapas, A.G., Hoenselaar, A., Keliris, G.A., and Logothetis, N.K., (2007) *Recording chronically from the same neurons in awake, behaving primates.* Journal of neurophysiology 98: pp. 3780-3790.

Vetter, R.J., Williams, J.C., Hetke, J.F., Nunamaker, E.A., and Kipke, D.R., (2004) *Chronic neural recording using silicon-substrate microelectrode arrays implanted in cerebral cortex.* IEEE Trans Biomed Eng 51 (6): pp. 896-904.